2008-06-25

Regulation of ROS signal transduction by NADPH oxidase 4 localization

Kai Chen
University of Massachusetts Medical School

Et al.

Published June 23, 2008

Regulation of ROS signal transduction by NADPH oxidase 4 localization

Kai Chen, Michael T. Kirber, Hui Xiao, Yu Yang, and John F. Keaney Jr.

Division of Cardiovascular Medicine, Department of Medicine, University of Massachusetts Medical School, Worcester, MA 01605

Reactive oxygen species (ROS) function as intracellular signaling molecules in a diverse range of biological processes. However, it is unclear how freely diffusible ROS dictate specific cellular responses. In this study, we demonstrate that nicotinamide adenine dinucleotide phosphate reduced oxidase 4 (Nox4), a major Nox isoform expressed in nonphagocytic cells, including vascular endothelium, is localized to the endoplasmic reticulum (ER). ER localization of Nox4 is critical for the regulation of protein tyrosine phosphatase (PTP) 1B, also an ER resident, through redox-mediated signaling. Nox4-mediated oxidation and inactivation of PTP1B in the ER serves as a regulatory switch for epidermal growth factor (EGF) receptor trafficking and specifically acts to terminate EGF signaling. Consistent with this notion, PTP1B oxidation could also be modulated by ER targeting of antioxidant enzymes but not their untargeted counterparts. These data indicate that the specificity of intracellular ROS-mediated signal transduction may be modulated by the localization of Nox isoforms within specific subcellular compartments.

Introduction

There is now considerable evidence indicating that reactive oxygen species (ROS) are involved in signal transduction. These species include the three successive reduction products of molecular oxygen such as superoxide ($^{\bullet}O_2-$), hydrogen peroxide (H_2O_2), and hydroxyl radical ($^{\bullet}OH$). Each of these species possesses chemical properties that potentially impact their signaling function. For example, OH• is the most unstable ROS with a half-life of 10^{-9} s (Pryor, 1986), indicating that it will react with any species within a radius of ~30 Å, thereby limiting its ability to transmit signals across any significant distance. Superoxide carries a negative charge that limits its membrane permeability to anion channels. In contrast, H_2O_2 is thought to be freely permeable and, thus, could react with several intra- and extracellular targets, limiting its specificity; however, this concept has recently been challenged (Branco et al., 2004). Thus, the chemical properties of ROS suggest significant limitations toward the production of specific cellular responses.

The prototypical NADPH oxidase (Nox) family member is Nox2 (also known as $gp91^{phox}$), which was initially found in phagocytes and plays a role in host defense by giving an outward burst of ROS (Cheng et al., 2001). Over the last several years, Nox2 along with its homologues, including Nox1, Nox3, Nox4, Nox5, Duox1, and Duox2, have been identified in nonphagocytes. It now appears that Noxs in nonphagocytes serve as a major source of intracellular ROS that play important signaling roles. However, the complexity of these isoforms in controlling ROS production is increasingly apparent because each isoform has its unique expression pattern, subcellular localization, and subunits requirement. The specific mechanisms for specific cell signaling responses are not known; therefore, the goal of this study is to examine the mechanisms of ROS signaling specificity.

Correspondence to Kai Chen: kai.chen@umassmed.edu

Abbreviations used in this paper: EGFR, EGF receptor; ERK, extracellular signal-regulated kinase; HAEC, human aortic endothelial cell; MEF, mouse embryonic fibroblast; MSP, mitochondrial signal peptide; NO, nitric oxide; NOS, NO synthase; Nox, NADPH oxidase; PTP, protein tyrosine phosphatase; ROS, reactive oxygen species; VE, vascular endothelial.

Results

Exogenous versus endogenous sources of ROS initiate distinct signaling responses

ROS are known to mediate a variety of cellular signaling pathways, and experiments in vitro typically use an exogenous source of ROS such as H_2O_2 to directly initiate signaling responses. However, one must consider that exogenous application of H_2O_2 may not adequately reflect authentic endogenous ROS signaling. Indeed, exogenous H_2O_2 produces broad signaling responses, including the activation of extracellular signal-regulated kinase (ERK), JNK, p38 MAPKs (Fig. 1 A), and Akt (Thomas et al., 2002). In contrast, the EGF-stimulated signaling response, which is known to be mediated by ROS in epithelial cells (Bae et al., 1997), was restricted to the mitogenic ERK pathway (Fig. 1 B) in endothelial cells. We found that EGF-induced

J. Cell Biol. Vol. 181 No. 7 1129–1139
www.jcb.org/cgi/doi/10.1083/jcb.200709049

Published June 23, 2008

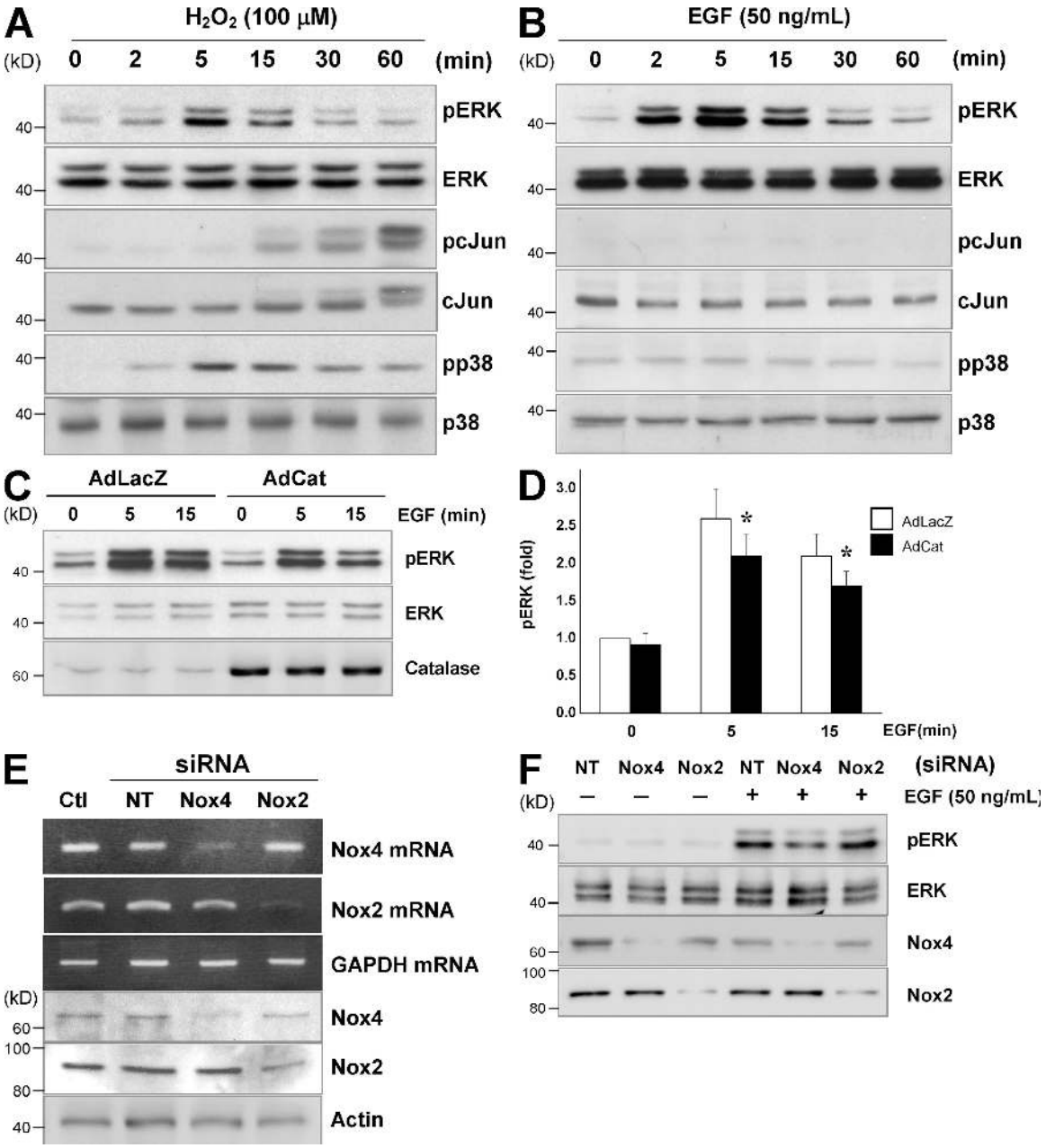

Figure 1. **A different source of ROS initiates distinct signaling responses in endothelial cells.** (A) HAECs were treated with 100 μM H_2O_2 for the indicated times, and total cell lysates were subjected to antibodies specific for pERK, ERK, pcJun, cJun, pp38, or p38. (B) HAECs were treated with 50 ng/ml EGF for the indicated times followed by immunoblotting with antibodies as in A. (C and D) Cells were treated with control adenovirus (Ad-LacZ) or catalase-overexpressing adenovirus (Ad-Cat) for 24 h before treatment with EGF followed by immunoblotting as in A. Error bars represent SD. *, $P < 0.05$. (E and F) HAECs were transfected with siRNA against nontargeting control (NT), Nox4, or Nox2 for 48 h before extraction of total RNA for RT-PCR and Western blotting (E) or treatment with EGF for 15 min followed by immunoblotting with pERK, ERK, Nox4, and Nox2 antibodies (F). Results are representative of four independent experiments.

ERK activation was attenuated by catalase overexpression (Fig. 1, C and D), indicating a role for ROS and a distinction between endogenous and exogenous ROS signaling.

To examine endogenous ROS responses in the endothelium, we suppressed the expression of Nox4 and Nox2, the two major Nox isoforms present in endothelial cells (Sorescu et al., 2002), using RNAi. As shown in Fig. 1 E, both Nox4 and Nox2 siRNA substantially reduced their respective mRNA and protein levels without cross-reactivity by >75% and 60%, respectively. We found that suppression of Nox4 attenuated ERK phosphorylation induced by EGF, whereas Nox2 suppression had no material impact (Fig. 1 F). Together, these data implicate endothelial Nox4 as an endogenous source of ROS in mediating EGF-induced signaling responses.

Nox4 is an ER-residing protein

To gain insight into the nature of Nox4, we examined its subcellular localization. The topography of Nox4 was examined in silico initially using PredictProtein (Columbia University), and it possesses six putative membrane-spanning regions, predicting

Published June 23, 2008

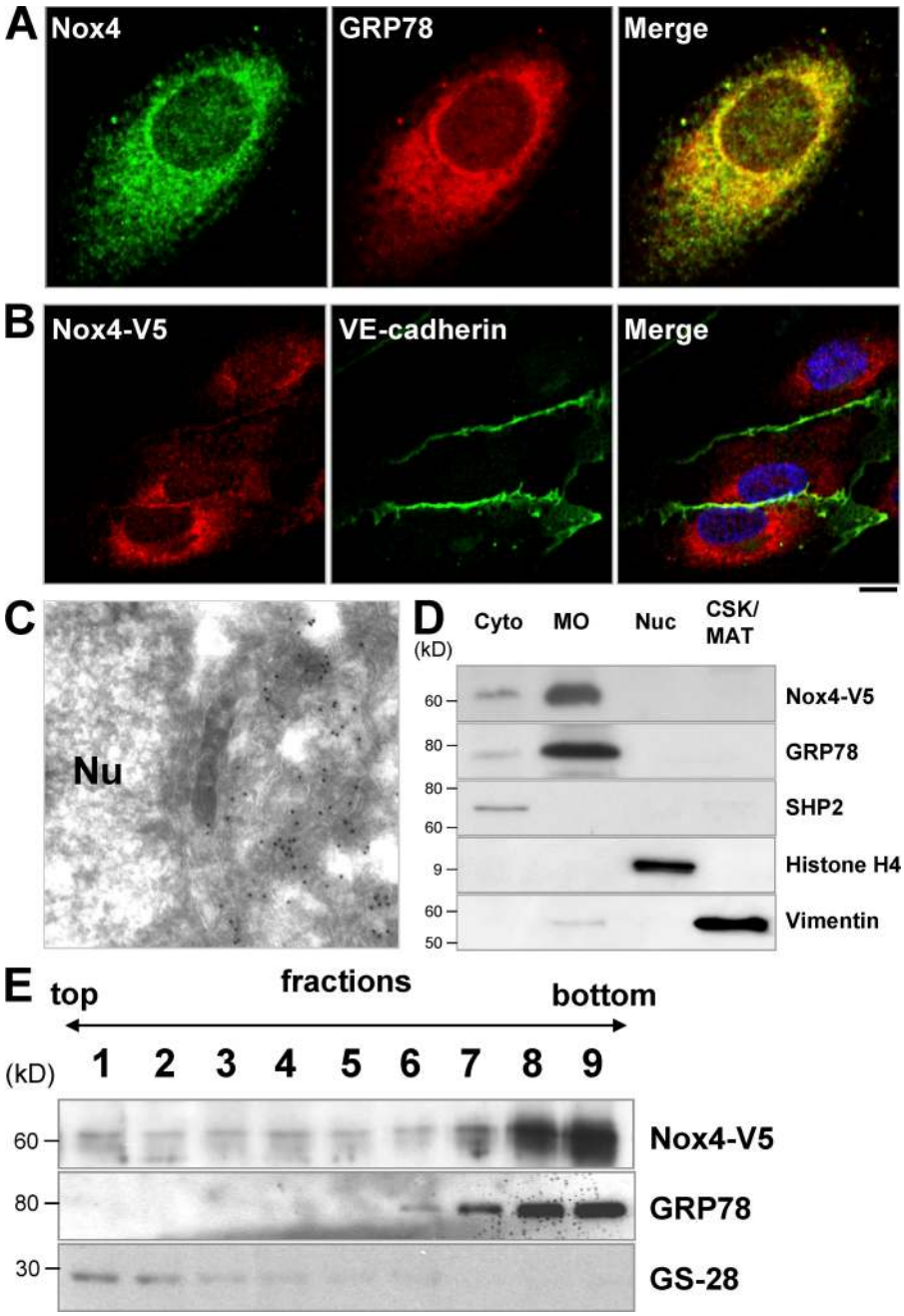

Figure 2. **Nox4 is localized to the ER.** (A) HAECs cultured in EBM2 medium were fixed and subjected to immunostaining with anti-Nox4 (AlexaFluor488; green) and anti-GRP78 (AlexaFluor594; red) followed by two-photon confocal microscopy. (B) HAECs were transfected with adenoviral vector expressing Nox4-V5 (AdNox4-V5). After 24 h, cells were probed with anti-V5 and VE-cadherin antibodies and visualized with AlexaFluor594 (red) and AlexaFluor488 (green), respectively. (C) Cells were transfected with AdNox4-V5 as in B followed by immunogold staining and were visualized by electron microscopy. (D and E) Similarly, HAECs with overexpression of Nox4-V5 were fractionated by biochemical detergent method (D) or Nycodenz gradient centrifugation (E). The obtained fractions cytosolic (Cyto), membrane/organelle (MO), nuclear (Nuc), and cytoskeletal/matrix (CSK/MAT) in D or fractions from top to bottom in E were subjected to immunoblotting with antibodies. Bars: (A) 5 μm; (B) 10 μm.

an integral membrane protein similar to Nox2. Further in silico analysis based on the Nox4 amino acid sequence using the PSORT II program (Human Genome Center, Tokyo University) and the *k*-nearest neighbor algorithm placed the probability of Nox4 localizing to the ER at 67%, whereas the probability of localization in plasma membrane, mitochondria, or the Golgi was only 11% each. Consistent with this prediction, confocal microscopy revealed a perinuclear distribution of endogenous Nox4 with colocalization with the ER marker protein GRP78 (Fig. 2 A). These data were confirmed using transfection with V5-tagged Nox4 by adenoviral vector in human aortic endothelial cells (HAECs; Fig. 2 B). There was no localization to the plasma membrane, as evident by staining for the plasma membrane marker vascular endothelial (VE) cadherin. Moreover, when COS-7 cells were examined after transfection with either V5- or myc-tagged Nox4, identical results were obtained regardless of whether the tag was C or N terminal (unpublished data). Finally, using immunogold electron microscopy in HAECs transfected with adenoviral V5-tagged Nox4 (Fig. 2 C), we observed gold particles predominantly in the ER membrane. To confirm the aforementioned results, a biochemical analysis of subcellular fractionation was performed in Nox4-V5–overexpressing cells and revealed that Nox4-V5 was mainly detected in the fraction of membrane/organelle that coincides with the ER marker GRP78 (Fig. 2 D) but not with other intracellular markers, including SHP-2 as a cytoplasmic marker, histone H4 as a nuclear marker, and vimentin as a cytoskeletal marker (Higashi et al., 2002). Similarly, analysis by nonlinear Nycodenz density gradient

Published June 23, 2008

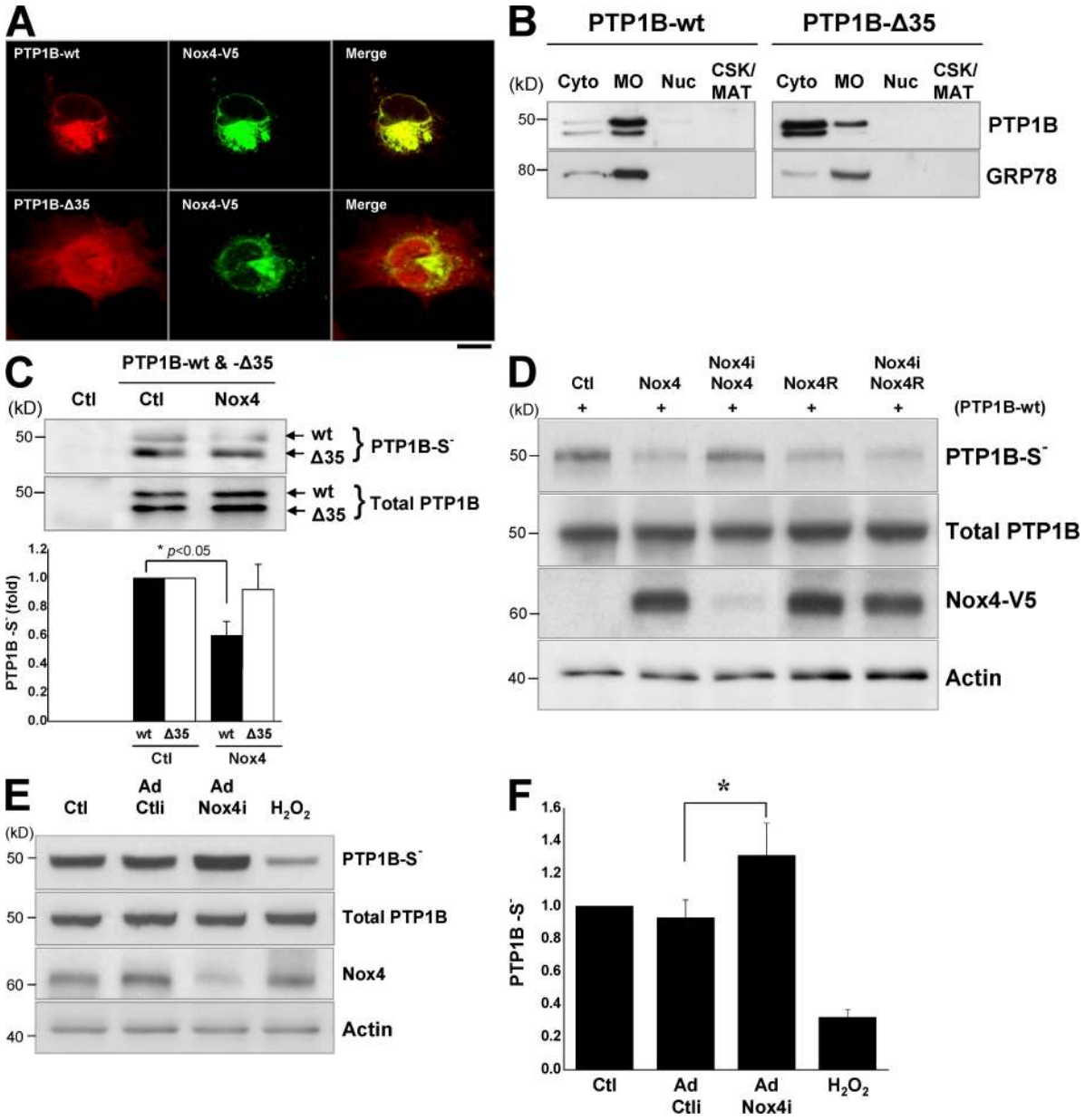

Figure 3. **PTP1B oxidation by Nox4 is spatially dependent.** (A) COS7 cells were transfected with pcDNA3.1/PTP1B wild type or pcDNA3.1/PTP1B-Δ35 in addition to pcDNA3.1/Nox4-V5. After 24 h, cells were fixed and immunostained with anti-V5 (green) for Nox4-V5 and anti-PTP1B for PTP1B wild type and C-terminal deleted PTP1B-Δ35 (red). (B) Cells transfected as in A were also subjected to detergent fractionation followed by immunoblotting with anti-PTP1B and anti-GRP78. Fractions include cytosolic (Cyto), membrane/organelle (MO), nuclear (Nuc), and cytoskeletal/matrix (CSK/MAT). (C) COS-7 cells treated as in A were lysed and labeled with biotin polyethylene oxide maleimide. Subsequent immunoprecipitation with avidin followed by immunoblotting with anti-PTP1B yields a band that represents the reduced, active form of PTP1B. (D) COS-7 cells were transfected with pcDNA3.1/Nox4-V5 or its Nox4i-resistant version pcDNA3.1/Nox4-R in combination with/without pQ/Nox4i. PTP1B oxidation was assessed as in C, and the efficiency of Nox4 knockdown was probed by V5. Total cellular PTP1B is shown in the bottom panel. (E and F) HAECs were transfected with Ad-control siRNA (Ad-Ctli) or Ad-Nox4i for 48 h before lysis and labeling with biotin polyethylene oxide maleimide. Treatment of cells with H_2O_2 at 100 μM for 5 min served as a positive control. Blots are representative of three independent experiments. Error bars represent SD. *, P < 0.05. Bar, 10 μm.

centrifugation revealed that Nox4-V5 is present in fractions that are enriched with the ER marker GRP78 but not the Golgi marker GS-28 (Fig. 2 E). Collectively, these data establish that Nox4 is localized to the ER of endothelial cells.

Nox4-dependent redox regulation of PTP1B requires colocalization

Signaling via ROS is thought to be mediated by regulation of the redox-sensitive cysteine of target proteins, including protein tyrosine phosphatases (PTPs). Because PTP1B is an ER-resident protein and its C-terminal 35 amino acid residues are critical for ER targeting (Frangioni et al., 1992; Salmeen et al., 2003; van Montfort et al., 2003), we first overexpressed PTP1B wild type (PTP1B) and a mutant lacking the C-terminal 35 amino acids (PTP1B-Δ35) in COS-7 cells and observed their distinct cellular localization. Although the wild-type PTP1B shows strong perinuclear colocalization with Nox4, the mutant PTP1B exhibits diffuse cytoplasmic distribution (Fig. 3 A) and predominant

Published June 23, 2008

relocation to the cytosol by detergent fractionation (Fig. 3 B). Other than the location, PTP1B-Δ35 has retained its enzymatic activity and indeed has shown a slightly higher activity compared with wild-type PTP1B (Frangioni et al., 1992). This property prompted us to determine whether PTP1B is subject to oxidative modification by Nox4 in a spatially dependent manner. Using the preceding cotransfection system, we assessed the PTP1B oxidation status with biotin maleimide as a function of cooverexpressed Nox4 level. Biotin maleimide irreversibly alkylates SH− groups on the active cysteine of PTP1B, and, therefore, its PTP1B incorporation reflects the amount of reduced PTP1B. As shown in Fig. 3 C, coexpression of Nox4 with both PTP1B wild type and PTP1B-Δ35 led to less reduced PTP1B (PTP1B-S^-) only in wild-type PTP1B, which is consistent with more oxidation. However, there was no material change in PTP1B-Δ35 oxidation with or without Nox4 overexpression (Fig. 3 C), suggesting that cytosolic PTP1B is not subject to oxidation by Nox4.

To further validate the Nox4-dependent PTP1B oxidation by rescue experiment, we constructed an RNAi-producing vector targeting wild-type Nox4 (pQ/Nox4i) and an RNAi-resistant Nox4 overexpression vector (pcDNA3.1/Nox4-R) containing silent mutations in the RNAi target region but encoding wild-type Nox4 protein. Immunoblot analysis verified that Nox4 from pcDNA3.1/Nox4-V5 could be efficiently knocked down by pQ/Nox4i, whereas pcDNA3.1/Nox4-R was indeed resistant to Nox4i. Further examination of PTP1B wild-type redox status revealed increased oxidation (less reduced form) in association with Nox4 overexpression, which was attenuated by the presence of Nox4i. In contrast, the effect of Nox4-R, the Nox4i-resistant version of wild-type Nox4, on PTP1B oxidation was equivalent to that of the wild-type Nox4 but was unaltered by Nox4i (Fig. 3 D), suggesting the specificity of Nox4i and consistency of Nox4-dependent PTP1B oxidation. To recapitulate this interaction in HAECs, we used Ad-Nox4i originated from pQ/Nox4i and found that suppression of Nox4 by RNAi in HAECs was associated with more of the reduced form of PTP1B (PTP1B-S^-), whereas H_2O_2 treatment attenuated the band intensity (Fig. 3, E and F), indicating the Nox4-dependent oxidation of PTP1B in endothelial cells. Together, these results further support the notion that colocalization is essential for redox-dependent regulation.

Nox4-dependent PTP1B oxidation is involved in EGFR dephosphorylation

One action of PTP1B is the negative regulation of multiple receptor tyrosine kinases, including the EGF receptor (EGFR; Flint et al., 1997; Liu and Chernoff, 1997), in part through receptor endocytosis to a dephosphorylation compartment within the ER (Haj et al., 2002). To probe Nox4 involvement in regulating EGFR phosphorylation, we initially transfected COS-7 cells with Nox4 and examined EGF-stimulated EGFR tyrosine phosphorylation. As shown in Fig. 4 A, EGF treatment produced early robust EGFR phosphorylation at 5 min, which was attenuated at 30 min. Overexpression of Nox4 enhanced the phosphorylation of both EGFR and downstream ERK at 30 min after EGF treatment with little impact on the early response, suggesting an involvement of Nox4 in EGFR signaling at the late phase. To determine whether the regulation of EGFR phosphorylation by Nox4 is mediated by PTP1B, we transfected COS-7 cells with PTP1B in the presence or absence of Nox4. Overexpression of PTP1B enhanced EGFR dephosphorylation at 30 min after EGF treatment. In contrast, the late component of EGFR (Fig. 4 B) and ERK (Fig. 4 C) phosphorylation was enhanced in cells with Nox4 overexpression compared with PTP1B alone. Concerning the presence of endogenous PTP1B in COS-7 cells, we further used immortalized $PTP1B^{-/-}$ mouse embryonic fibroblasts (MEFs) along with $PTP1B^{-/-(+WT)}$ MEFs in which PTP1B has been reconstituted in $PTP1B^{-/-}$ MEFs. Consistent with the findings in COS-7 cells, Nox4 overexpression prolonged EGFR phosphorylation in $PTP1B^{-/-(+WT)}$ MEFs (Fig. 4 D). These results suggest Nox4-mediated regulation of EGFR dephosphorylation via PTP1B.

To address the spatial requirements of Nox4 in regulating EGFR signaling, we overexpressed PTP1B-Δ35 (Frangioni et al., 1993) and observed reduced EGFR phosphorylation (Fig. 4 B). However, Nox4 overexpression did not modify the effect of PTP1B-Δ35 on EGFR dephosphorylation and subsequent ERK activation status (Fig. 4 C). Further study with the cotransfection of Nox4 and PTP1B wild type/PTP1B-Δ35 in $PTP1B^{-/-}$ MEFs supported PTP1B wild type being the target of Nox4 in regulation of EGFR dephosphorylation (Fig. 4 E). In contrast, Nox4 was not effective in modulating the effect of PTP1B-Δ35 (Fig. 4 B). Thus, these data support the notion that colocalization of PTP1B and Nox4 in the ER is essential for redox regulation of EGFR signaling in various cell types, including endothelial cells (Fig. 4 F).

Oxidation of PTP1B trapping mutant by Nox4 attenuates its substrate-binding capacity

To gain insight into the mechanism of Nox4-mediated modulation of PTP1B activity, we used substrate-trapping PTP1B mutant that retains substrate-binding activity but cannot complete the catalytic cycle and release the substrate (Tonks, 2003). Indeed, COS-7 cell transfection with the PTPT1B trapping mutant (D181A/Q262A) produces an increase in phosphorylation of the EGFR that is enhanced after treatment with EGF (Fig. 5 A). Because the mutant PTP1B(D181A/Q262A) features disrupted trapping ability upon oxidation (Salmeen et al., 2003), we then sought to evaluate the involvement of Nox4-derived ROS in this setting. Overexpression of Nox4 in this system attenuated EGFR tyrosine phosphorylation at basal condition and after EGF stimulation (Fig. 5 A). The localization of EGFR visualized by using an enhanced GFP-EGFR expression vector was consistent with EGFR mobilization to the ER induced by PTP1B(D181A/Q262A) as a result of substrate trapping, which was reversed by Nox4 overexpression (Fig. 5 B). In agreement with this observation, the interaction between EGFR and PTP1B(D181A/Q262A) was evident but greatly attenuated by the presence of Nox4 as determined by pull-down assay (Fig. 5 C). Thus, these data suggest that Nox4-derived ROS mediate the oxidation status/trapping ability of PTP1B(D181A/Q262A) in relation to EGFR.

Published June 23, 2008

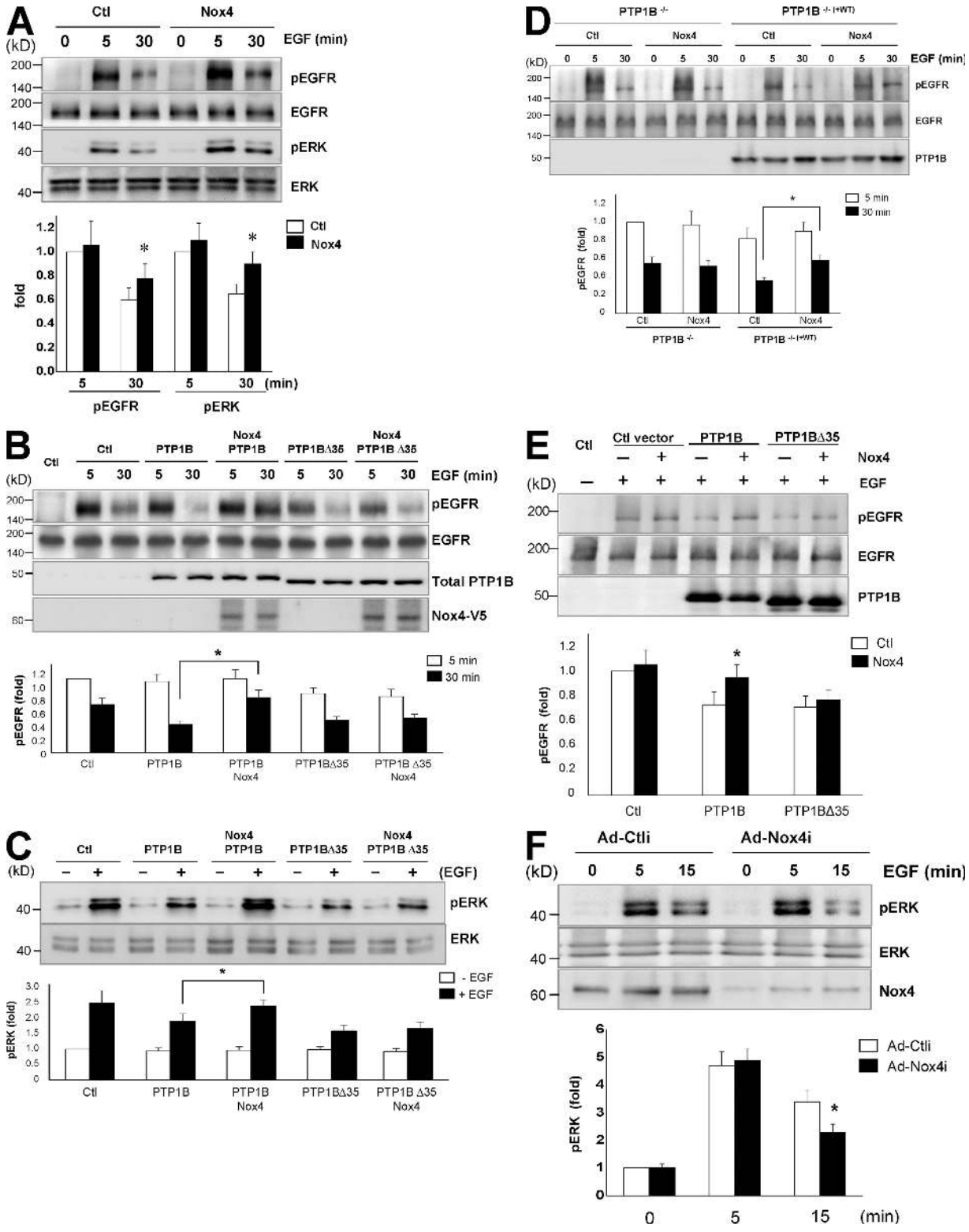

Figure 4. **Nox4-dependent PTP1B oxidation regulates EGF signaling.** (A) COS-7 cells were transfected with pcDNA3.1/Nox4-V5 for 24 h followed by 50 ng/ml EGF treatment for the indicated times. The lysates were probed for phosphorylated and total EGFR and ERK. *, $P < 0.05$ compared with the respective control. (B) COS-7 cells were transfected with pcDNA3.1/PTP1B or pcDNA3.1/PTP1B-Δ35 in addition to pcDNA3.1/Nox4-V5 and treated as in A. Phosphorylation of EGFR was determined by immunoprecipitation with anti-EGFR followed by immunoblotting with antiphosphotyrosine. Total PTP1B and Nox4 levels were examined by using anti-PTP1B and anti-V5, respectively. (C) ERK phosphorylation was measured at 30 min after EGF treatment by immunoblotting with antiphospho-ERK. (D) PTP1B$^{-/-}$ and PTP1B$^{-/-(+WT)}$ MEFs were transfected with or without pcDNA3.1/Nox4 followed by treatment and detection as in B. (B–D) *, $P < 0.05$. (E) PTP1B$^{-/-}$ MEFs were transfected with pcDNA3.1/PTP1B or pcDNA3.1/PTP1B-Δ35 in addition to pcDNA3.1/Nox4. Cells were collected for assay as in B. *, $P < 0.05$ compared with the respective control. (F) HAECs were transfected with Ad-control siRNA (Ad-Ctli) or Ad-Nox4i for 48 h and were treated with EGF for the indicated times. Phospho-ERK, total ERK, and Nox4 were determined. *, $P < 0.05$ compared with the respective Ad-Ctli. The blots are representative of three independent experiments. Error bars represent SD.

Published June 23, 2008

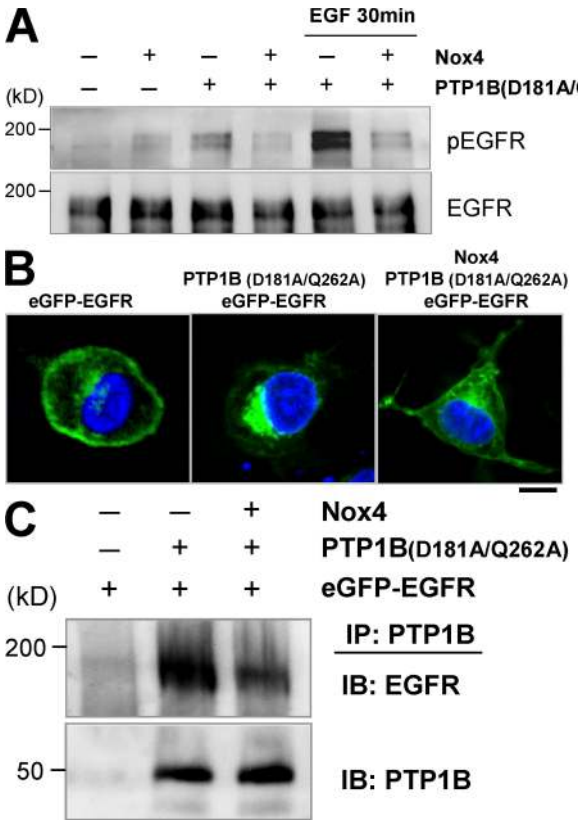

Figure 5. **Oxidation of PTP1B trapping mutant by Nox4 attenuates its substrate-binding capacity.** (A) COS-7 cells were transfected with expression vectors as indicated for 24 h followed by treatment with or without 50 ng/ml EGF for 30 min. Cell lysates were immunoprecipitated with EGFR antibody and immunoblotted with antiphosphotyrosine. Total cell lysates were also immunoblotted with anti-EGFR as shown in the bottom panel. (B) COS-7 cells were cultured on the glass coverslips and transfected with expression vectors as indicated for 24 h. Imaging was visualized with a two-photon confocal microscope. (C) COS-7 cells were treated as in B, and cell lysates were immunoprecipitated with PTP1B antibody followed by immunoblotting with anti-EGFR and anti-PTP1B. Bar, 10 μm.

ER-targeting antioxidants attenuate Nox4-derived ROS signaling

If ER localization is critical for Nox4 to modulate EGFR signaling, one might expect that ER targeting of antioxidants could attenuate the effect of Nox4. To test this hypothesis, we used the N-terminal 35 amino acid residues (N35) of Nox4 that confer ER localization (Fig. 6 A) to target catalase (N35-Cat) to the ER. N35-Cat exhibits perinuclear ER distribution distinct from its original peroxisomal sites (Fig. 6 B). We chose to use intracellular organelles targeting catalases for spatial-dependent manipulation because overexpression of wild-type catalase might leak into other intracellular compartments, including the ER, that might not be clean systems. We found that COS-7 cells transfected with catalase targeted to the ER (N35-Cat) or mitochondria (mitochondrial signal peptide [MSP]–Cat; Fig. 6 B; Bai et al., 1999) exhibited increased catalase activity (Fig. 6 C), but only N35-Cat and not MSP-Cat attenuated Nox4 modulation of EGFR signaling (Fig. 6 D). These results demonstrated the effectiveness of ER-targeting antioxidants in regulating ER-localized Nox4 ROS signaling.

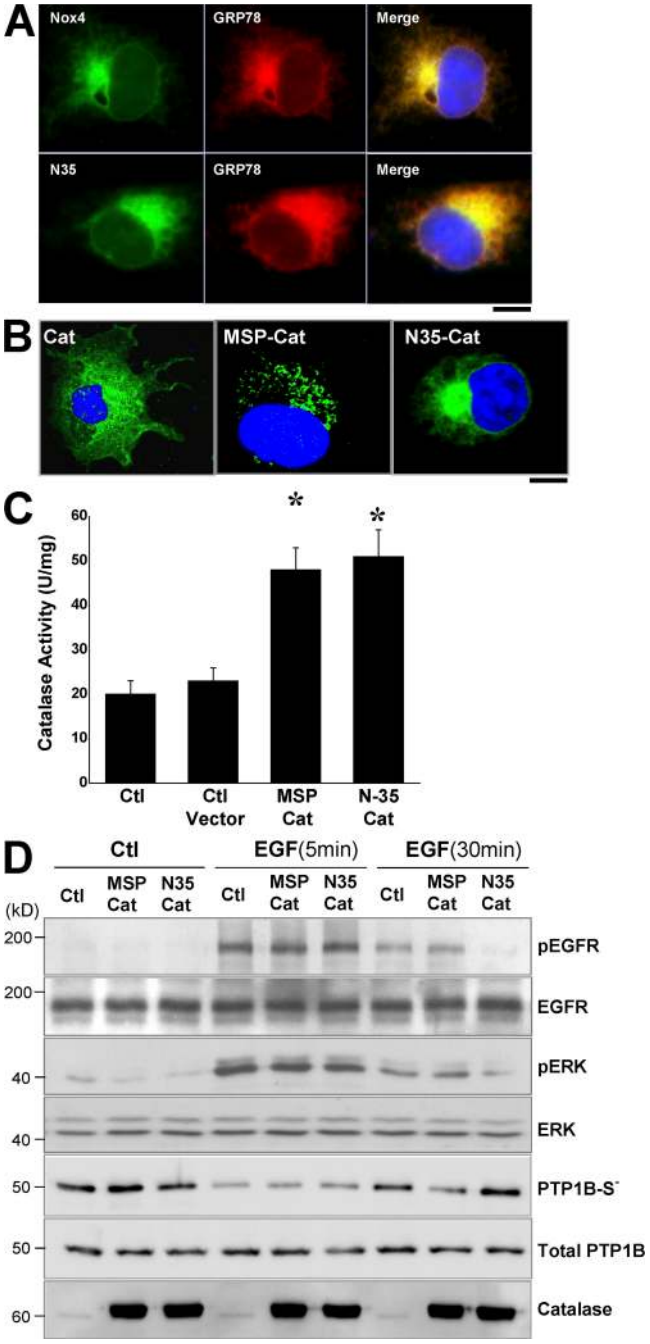

Figure 6. **ER-targeting antioxidant attenuates Nox4-dependent ROS signaling.** (A) COS-7 cells on coverslips were transfected with pcDNA3.1/Nox4-V5 or pcDNA3.1/N35-V5. After 24 h, cells were fixed and immunostained with anti-V5 (green) for fusion proteins and anti-GRP78 (red). (B) COS-7 cells were transfected with overexpression vectors as indicated and were immunostained with anticatalase antibodies. (C) COS-7 cells were transfected with mitochondrial-targeting catalase (MSP-Cat) or ER-targeting catalase (N35-Cat) as indicated for 24 h. Catalase activity was measured in cell lysates using the Amplex red catalase kit. Error bars represent SD. *, $P < 0.05$ versus control. (D) The Nox4-overexpressing COS-7 cell line was transfected with pcDNA3.1/PTP1B in combination with either MSP-catalase or N35-catalase. After 24 h, cells were treated with 50 ng/ml EGF, and phosphorylation of EGFR and ERK and PTP1B oxidation status were determined as described in Materials and methods. The blots are representative of three independent experiments. Bars, 10 μm.

Published June 23, 2008

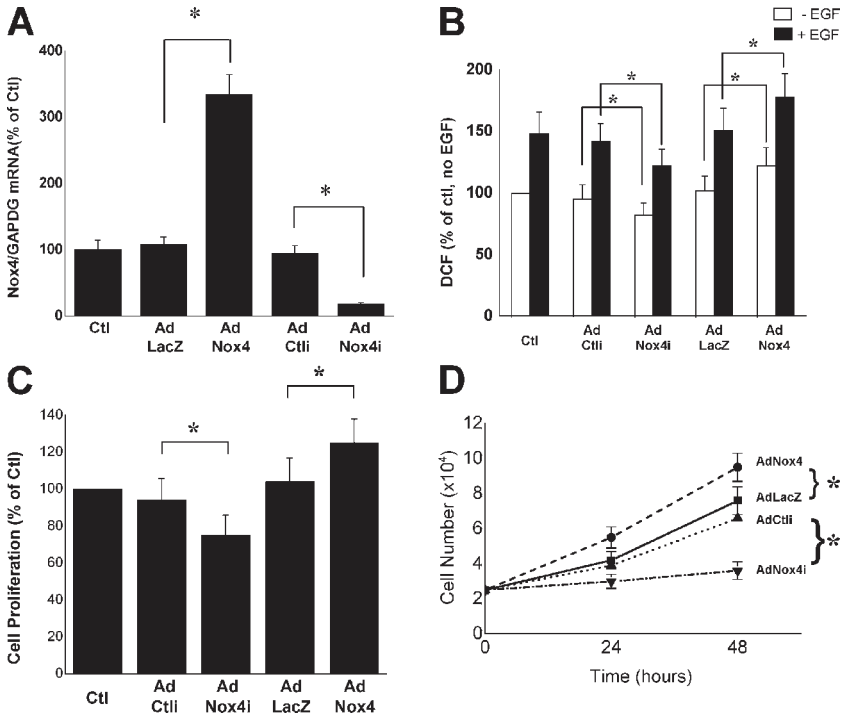

Figure 7. **EGF-induced endothelial proliferation is mediated by Nox4-dependent PTP1B oxidation.** HAECs were transfected with Ad-control siRNA (Ad-Ctli) or Ad-Nox4i for 48 h or adenoviral vectors expressing LacZ (AdLacZ)/Nox4 (AdNox4) for 24 h. (A and B) Total RNA was extracted followed by RT-PCR for measurement of Nox4 mRNA (A) and dichlorofluorescein assay for ROS production in response to 50 ng/ml EGF for 15 min (B). For proliferation assay, HAECs were transfected with adenoviral vectors as in A for 24 h and were seeded into 24-well plates at 2.5×10^4 cells/well. (C and D) Proliferation was measured by BrdU incorporation (C), and cell number was counted at 24 and 48 h after plating (D). Data are shown as representative (gel picture) or statistics of three independent experiments. Error bars represent SD. *, $P < 0.05$.

EGF-induced endothelial proliferation is mediated by Nox4-dependent PTP1B oxidation

To examine the functional implications of Nox4 in EGF-dependent endothelial cell responses, we manipulated the endothelial Nox4 levels using adenoviral overexpression and RNAi. Both strategies resulted in significant changes in Nox4 expression at the mRNA level (Fig. 7 A), and EGF-induced ROS production in these cells was correlated with Nox4 expression (Fig. 7 B). Furthermore, EGF-stimulated endothelial cell proliferation as determined by either BrdU incorporation (Fig. 7 C) or cell counting (Fig. 7 D) was consistently enhanced by the overexpression of Nox4. Conversely, RNAi-mediated suppression of Nox4 attenuated cell proliferation. Collectively, these data indicate that Nox4-derived ROS play an important role in regulating PTP1B oxidation and EGF signaling in a manner that modulates cell proliferation.

Discussion

The principal finding of this study is that endothelial Nox4, an endogenous source of ROS in HAECs, is localized to the ER and appears involved in the regulation of another ER-residing protein, PTP1B, in a spatially dependent manner. Despite the diffusible nature of H_2O_2, Nox4-dependent oxidative modification of PTP1B requires colocalization of both proteins in the ER. We found that cytosolic PTP1B prevented its oxidation by Nox4. Furthermore, we found that Nox4-mediated PTP1B oxidation was relevant to EGF signaling and was associated with reduced dephosphorylation of EGFR in proximity to the ER. We were able to confirm the importance of ER localization using ER targeting of antioxidant enzymes such as catalase. Collectively, these data provide a paradigm for Nox4-dependent redox signaling that highlights spatial specificity within the cell.

The notion that ROS are involved in cell signaling is not new (Finkel and Holbrook, 2000), and the diffusible nature of H_2O_2 is thought to be consistent with this role. In this regard, previous experience with nitric oxide (NO) merits particular attention. For example, NO was thought to readily diffuse to its effector site, making its site of generation irrelevant. However, it is now clear that cell responses vary dramatically depending on the site of the NO synthase (NOS) enzymes. For example, NOS1 in the sarcoplasmic reticulum of cardiomyocytes regulates ryanodine receptor Ca^{2+} release, whereas NOS3 in caveolae regulates L-type Ca^{2+} channels (Barouch et al., 2002). The ER localization of Nox4 may have some advantages for redox-related signal transduction as a result of the relatively oxidized state of the ER (Tu and Weissman, 2004). The low antioxidative capacity in the region may allow Nox4 to initiate signaling more efficiently or cause pathological events while dysregulated. Consistent with this notion, Nox4 has recently been related to ER stress and apoptosis in 7-ketocholesterol–treated human aortic smooth muscle cells (Pedruzzi et al., 2004). The data presented here underlines the importance of subcellular localization as a regulatory theme in redox signaling.

PTP1B is localized exclusively on the cytoplasmic face of the ER and contains a small hydrophobic C-terminal anchor sequence that is necessary and sufficient to localize the enzyme to the ER (Frangioni et al., 1992). Haj et al. (2002) demonstrated that the activated EGFR is internalized and transported to the ER, where it is subject to dephosphorylation by PTP1B. The catalytic activity of PTPs is dependent on a reduced active site Cys residue, and the catalytic Cys is extremely susceptible to oxidation by H_2O_2 (Meng et al., 2002). Here, we demonstrate that Nox4 is a source of H_2O_2 that modulates the PTP1B redox state and, as a consequence, the duration of EGFR signaling. Modulating the duration of EGFR signaling had functional consequences, as

Published June 23, 2008

both downstream ERK signaling and endothelial cell proliferation were subject to Nox4-mediated control. Insofar as receptor tyrosine kinase transport to sites of dephosphorylation is shared among receptors, one might speculate that our observations represent a general mechanism for regulating the duration of receptor tyrosine kinase activity. Indeed, most studies of ROS signaling have found only partial modulation of signaling rather than a strict dependence of responses by manipulating ROS. For example, a previous study demonstrated limited inhibition of angiotensin-induced ERK activation by antioxidants tempol or tiron in vascular smooth muscle cells exposed to angiotensin for 5 min (Touyz et al., 2004). Nevertheless, tempol has shown significant reduction in angiotensin-induced aortic vascular hypertrophy in mouse models, which tends to support the new paradigm (Dikalova et al., 2005).

The data presented here indicate that ROS-mediated signaling responses are compartmentalized. Consistent with this notion, EGF treatment has been shown to cause only selective oxidation of the subcellularly localized thioredoxin pool but has no material impact on the intracellular glutathione/glutathione disulfide redox pool (Halvey et al., 2005). The precise mechanisms of this signaling compartmentalization are not yet known but may be maintained through either membrane barrier function and/or localization of antioxidant capacity close to the ROS source. Indeed, our observations with ER-targeted antioxidants tend to support the latter possibility. This contention is consistent with the observation that compared with cytosol or mitochondria-targeting peroxiredoxin 5, only nucleus-targeting peroxiredoxin 5 confers DNA protection from oxidative injury (Banmeyer et al., 2004). However, it remains unknown which intracellular antioxidants might perform this function in the context of the Nox4 system.

The functional implications of Nox4 have been diverse, including antiproliferative effects in NIH3T3 cells (Geiszt et al., 2000; Shiose et al., 2001), proliferative effects in smooth muscle cells (Menshikov et al., 2006), maintenance of a differentiated smooth muscle cell phenotype (Clempus et al., 2007), and modulation of insulin signaling in adipocytes (Mahadev et al., 2004). The proliferative effect of Nox4 in endothelial cells suggests a common signaling role of intracellular ROS in nonphagocytic cells. This finding is in agreement with previous studies indicating that ROS mediates peptide growth factor–induced signaling and increased cell growth (Sundaresan et al., 1995; Bae et al., 1997). As an important intracellular ROS source, Nox1 was the first enzyme among the members of the Nox family found to participate in physiological mitogenesis in response to growth factors (such as platelet-derived growth factor) as well as pathological hyperproliferation (such as cancer and atherosclerosis; Suh et al., 1999). However, the assumption of Nox4 being proliferative turned out to be untrue in early studies using overexpression strategy in NIH3T3 fibroblasts (Shiose et al., 2001). In agreement with our results, the depletion of Nox4 resulted in a significantly decreased rate of proliferation in melanoma, pancreatic cancer, and vascular smooth muscle cells (Brar et al., 2002; Vaquero et al., 2004; Djordjevic et al., 2005). Although the reasons for the difference from these studies are not clear, an important clue to the biological function of Nox4 links to its subcellular location.

The intracellular localization of Nox4 remains controversial. Hilenski et al. (2004) reported Nox4 in the nucleus and focal adhesion sites in rat vascular smooth muscle cells, whereas other studies revealed perinuclear or nuclear distribution in COS-7, HEK293, and endothelial cells (Kuroda et al., 2005; Martyn et al., 2006; Petry et al., 2006). It may not be surprising if different cell types display distinct intracellular localization of the same protein. However, a recent study that showed nuclear localization of Nox4 in human VE cells (Kuroda et al., 2005) conflicts with the results here. Although the reason for the discrepancy remains unclear, one explanation may be related to the antibodies used in the study by Kuroda et al. (2005), in which antibodies were generated solely targeting the C terminus of Nox4. It is plausible that these antibodies may recognize certain splice variants of Nox4 because two out of four different splice variants have been found to be predominantly C-terminal truncated forms (Goyal et al., 2005). Of note, we have constructed such a truncated form of Nox4 (amino acids 418–578) and observed a nuclear localization (unpublished data).

The current findings demonstrate a new biological paradigm for ROS signaling whereby the spatial confinement of ROS with redox-sensitive targets in proximity allows ROS signals to keep targeting selectivity. As such, ROS oxidatively fine-tune the PTP1B activity in this system that subsequently regulates receptor trafficking. In addition, we have shown the effectiveness of ER-targeting catalase in the regulation of Nox4, a finding that implicates the importance of manipulating ROS within specific intracellular microdomains to ensure the effects. This may partially explain the failure of antioxidants as therapeutic agents in a series of clinical trials and points out the relevance of manipulation at the subcellular level. ROS signaling appears to be operated in a spatially restricted microenvironment with substrate specificity. It is worth noting that the Nox4-dependent PTP oxidative modification was evident across multiple cell types and held true for the regulatory mechanism of other different receptors, including the insulin receptor. Our data may provide a model for numerous redox-sensitive signaling systems and have broad-ranging implications in cardiovascular diseases and cancer.

Materials and methods

Materials

A rabbit polyclonal antibody was raised against human Nox4 in our laboratory (Wendt et al., 2005). Anti-EGFR, GS-28, SHP-2, and VE-cadherin were purchased from Santa Cruz Biotechnology, Inc. Anti-GRP78 was obtained from BD Biosciences, anticatalase and anti–histone H4 were obtained from Abcam, antivimentin was purchased from NeoMarkers, and anti-V5, AlexaFluor488-, and AlexaFluor594-conjugated secondary antibodies were obtained from Invitrogen. Phosphotyrosine antibody (4G10) was obtained from Millipore, and all MAPK antibodies were purchased from Cell Signaling Technology. Human recombinant EGF, anti-PTP1B, and a BrdU cell proliferation assay kit were purchased from EMD. All other reagents were obtained from Sigma-Aldrich. Double-stranded siRNAs for Nox4, Nox2, and nontargeting control were obtained from Dharmacon.

Cell culture

HAECs were obtained and cultured in EGM-2 (Cambrex) as described previously (Chen et al., 2001). COS-7 cells were purchased from the American Type Culture Collection and maintained in DME supplemented with 10% FBS. The COS-Nox4 cell line was established by transfection of pcDNA3.1/Nox4-V5 in COS-7 cells followed by G418 selection. Immortalized PTP1B$^{-/-}$ primary MEFs (PTP1B$^{-/-}$ MEFs) and PTP1B$^{-/-}$ MEFs

Published June 23, 2008

reconstituted with wild-type PTP1B (PTP1B$^{-/-(+WT)}$ MEFs) were provided by B. Neel (Harvard Medical School, Boston, MA; Haj et al., 2003).

Plasmid constructs and adenoviral vectors

CFP-EGFR and enhanced GFP-EGFR expression vectors were provided by L. Samelson (National Institutes of Health, Bethesda, MD) and T. Jovin (Max Planck Institute, Göttingen, Germany), respectively. pZeoSV2/MSP-catalase vector was a gift from J. Andres Melendez (Albany Medical College, Albany, NY). PTP1B vectors, including wild-type and mutant D181A/Q262A, were provided by Z.-Y. Zhang (Indiana University, Bloomington, IN). Expression vectors pcDNA3.1/Nox4-V5, pcDNA3.1/PTP1B wild type, pcDNA3.1/PTP1B-Δ35, pcDNA6.2/EmGFP-PTP1B (D181A/Q262A), pcDNA3.1/SOD1, and pcDNA3.1/catalase were constructed by using the PCR subcloning technique with pcDNA3.1/TOPO-V5 or pcDNA6.2/EmGFP vectors (Invitrogen). Adenoviral Nox4 vector was a gift from B. Goldstein (Thomas Jefferson University, Philadelphia, PA). For the generation of AdNox4-V5, full-length human Nox4 cDNA was subcloned into pENTR/D-TOPO vector (Invitrogen) followed by recombination reaction with pAd/CMV/V5-DEST (Invitrogen). The resulting clone was used for the generation of adenoviral stock in 293A cells, and further purification was performed with cesium chloride ultracentrifugation. An MOI of 50 was used throughout the experiments. For generation of Nox4-targeting RNAi vector pQ/Nox4i, a sequence targeting Nox4 (nucleotides 418–436 of human Nox4 from the start codon) was constructed within pQuiet-U6 vector (Welgen). The construct was also ligated into a linearized adenoviral genome for subsequent generation of adenoviral vector (Ad-Nox4i). To generate a Nox4-overexpressing vector (pcDNA3.1/Nox4-R) that is specifically resistant to the corresponding pQ/Nox4i for rescue experiments, eight silent mutations were introduced into a parental pcDNA3.1/Nox4-V5 at the Nox4i target region without altering the encoding protein by using the QuikChange Site-Directed Mutagenesis kit (Stratagene).

Plasmid and siRNA transfection

COS-7 cells were seeded at a density of 2×10^5 cells/ml in 6-well plates. Transfection with overexpression plasmids was performed using Fugene 6 (Roche) in cells at 70% confluency according to the manufacturer's instructions. Typically, 2 µg of plasmid per well was used for transfection, and cells were ready for experiments 24 h later. Transfection in PTP1B$^{-/-}$ MEFs was performed by using Lipofectamine 2000 (Invitrogen). Transfection of HAECs with siRNA was performed using the TransMessenger Transfection Reagent (QIAGEN) according to the manufacturer's instructions. Cells were incubated for 48 h after siRNA transfection before experiments.

Immunoprecipitation and Western blotting

Immunoprecipitation and Western blotting procedures were performed as previously described (Chen et al., 2001). Densitometric analysis of immunoblots was performed using ImageJ software (National Institutes of Health).

Detergent fractionation of subcellular organelles

Cell fractions were extracted by using the differential detergent fractionation method as described previously (Simpson, 2003). In brief, the detergent fractionation involves the sequential extraction of cells with Pipes buffers containing 0.015% digitonin, then 0.5% Triton X-100, and finally 1% Tween 40/0.5% deoxycholate, yielding three biochemically and electrophoretically distinct fractions composed of cytosolic, membrane/organelle, and nuclear compartments, respectively. The final cell residue from the aforementioned procedures was the detergent-resistant cytoskeletal/matrix compartment.

Nycodenz fractionation of subcellular organelles

Nycodenz gradient fractionation was performed essentially as described previously (Hammond and Helenius, 1994). Cells were harvested and homogenized in 2 ml of ice-cold homogenizing buffer (10 mM Tris-HCl, pH 7.4, 250 mM sucrose, 5 mM EDTA, and protease inhibitor mixture). Postnuclear supernatant was obtained (3,000 rpm for 10 min at 4°C), and a step gradient was created in centrifuge tubes (TLS-55; Beckman Coulter) by loading top to bottom 0.5 ml of 10, 14.66, 19.33, and 24% Nycodenz solution in saline buffer. The postnuclear supernatant was then layered on top of the gradient and fractionated by centrifugation (169,000 *g* for 45 min at 15°C). After centrifugation, fractions were collected from the top of the tube, and an aliquot of each fraction was resolved by SDS-PAGE and Western blot analysis.

Immunofluorescence

Cells were grown on glass cover slides and fixed with 4% PFA. Primary antibodies were diluted at 1:250, and secondary antibodies include Alexa-Fluor488 or -594 goat anti–rabbit or mouse IgG (Invitrogen) at 1:200 dilution. Fluorescence images were obtained using a 40× 1.30 oil objective (Nikon) on an inverted microscope (TE-2000; Nikon) with a camera (CoolSNAP HQ; Photometrics). Images were captured using NIS-Elements software (Nikon) and processed with a 3D deconvolution plug-in (MediaCybernetics).

Immunogold electron microscopy

HAECs were transfected with adenoviral vector expressing Nox4-V5 for 24 h and were removed from the dish with 0.5 mM EDTA in PBS. The cell suspension was layered on top of a cushion of 4% PFA and pelleted for 3 min at 3,000 rpm. The pellet was further fixed in fresh 4% PFA for 2 h followed by wash with PBS containing 0.2 M glycine and infiltration with 2.3 M sucrose. Frozen samples were sectioned and subjected to anti-V5 (1:100) followed by protein A gold labeling. The grids were examined in a transmission electron microscope (Harvard Medical School EM Facility; 1200EX; JEOL).

Detection of PTP1B redox state

For detection of PTP1B at a reduced form (SH-PTP1B), cells were lysed on ice for 10 min in lysis buffer containing 1 mM biotin polyethylene oxide maleimide (Thermo Fisher Scientific) followed by precipitation with UltraLink Immobilized NeutrAvidin (Thermo Fisher Scientific) and Western blot analysis with PTP1B antibody (Lee et al., 2002). The band detected here represents the amount of PTP1B at a reduced form.

RT-PCR analysis

Extraction of total RNA and RT-PCR was performed as previously described (Chen et al., 2003). The forward and reverse primers corresponding to Nox4, Nox2, and glyceraldehyde-3-phosphate dehydrogenase were 5′-AAGCCGGAGAACCAGAAGAT-3′ and 5′-GCTGCATTCAGTTCGACAAA-3′ for Nox4, 5′-GCTTGTGGCTGTGATAAGCA-3′ and 5′-TCCCTGCTCCCACTAACATC-3′ for Nox2, and 5′-ACCCAGAAGACTGTGGATGG-3′ and 5′-AGGCCATGCCAGTGAGCTT-3′ for glyceraldehyde-3-phosphate dehydrogenase.

Measurement of ROS

Intracellular ROS production was measured by dichlorofluorescein fluorescence as described previously (Chen et al., 2000). Cells cultured in 6-well plates were changed to Hepes-buffered physiological saline solution followed by the addition of 5 µM H2DCFH-DA with/without EGF treatment and further incubation for 20 min at 37°C. After treatment and wash, fluorescence intensity was quantified by using a fluorescence plate reader (SpectraMax GeminMPS; MDS Analytical Technologies).

Catalase activity assay

Cells were transfected with control vector or catalase expression vectors for 24 h and lysed in 0.1 M Tris buffer, pH 7.4. Cell lysates were used for measurement of catalase activity by using the Amplex Red Catalase Assay kit (Invitrogen). The decomposition of hydrogen peroxide by catalase was followed by reaction with 50 µM Amplex red reagent in the presence of 0.2 U/ml horseradish peroxidase. Fluorescence was measured in a fluorescence microplate reader (MDS Analytical Technologies) using excitation at 530 nm and emission at 590 nm.

Statistical analysis

All numerical data are presented as means ± SD. The Western blots shown are representative of three or more independent experiments. For parametric data, comparisons among treatment groups were performed with one-way analysis of variance and an appropriate posthoc comparison. Instances involving only two comparisons were evaluated with a *t* test. Instances involving more than two comparisons were evaluated using analysis of variance. Statistical significance was accepted if the null hypothesis was rejected with $P < 0.05$.

We are grateful to Yongmei Pei, Xiaoyun Huang, and Adam Albano for their technical assistance.

K. Chen is the recipient of a Scientist Development grant from the American Heart Association, and this work was partially supported by National Institutes of Health grant AG027081 to J.F. Keaney Jr.

Submitted: 10 September 2007
Accepted: 27 May 2008

References

Bae, Y.S., S.W. Kang, M.S. Seo, I.C. Baines, E. Tekle, P.B. Chock, and S.G. Rhee. 1997. Epidermal growth factor (EGF)-induced generation of

hydrogen peroxide. Role in EGF receptor-mediated tyrosine phosphorylation. *J. Biol. Chem.* 272:217–221.

Bai, J., A.M. Rodriguez, J.A. Melendez, and A.I. Cederbaum. 1999. Overexpression of catalase in cytosolic or mitochondrial compartment protects HepG2 cells against oxidative injury. *J. Biol. Chem.* 274:26217–26224.

Banmeyer, I., C. Marchand, C. Verhaeghe, B. Vucic, J.F. Rees, and B. Knoops. 2004. Overexpression of human peroxiredoxin 5 in subcellular compartments of Chinese hamster ovary cells: effects on cytotoxicity and DNA damage caused by peroxides. *Free Radic. Biol. Med.* 36:65–77.

Barouch, L.A., R.W. Harrison, M.W. Skaf, G.O. Rosas, T.P. Cappola, Z.A. Kobeissi, I.A. Hobai, C.A. Lemmon, A.L. Burnett, B. O'Rourke, et al. 2002. Nitric oxide regulates the heart by spatial confinement of nitric oxide synthase isoforms. *Nature.* 416:337–339.

Branco, M.R., H.S. Marinho, L. Cyrne, and F. Antunes. 2004. Decrease of H2O2 plasma membrane permeability during adaptation to H2O2 in *Saccharomyces cerevisiae*. *J. Biol. Chem.* 279:6501–6506.

Brar, S.S., T.P. Kennedy, A.B. Sturrock, T.P. Huecksteadt, M.T. Quinn, A.R. Whorton, and J.R. Hoidal. 2002. An NAD(P)H oxidase regulates growth and transcription in melanoma cells. *Am. J. Physiol. Cell Physiol.* 282:C1212–C1224.

Chen, K., K. Gunter, and M.D. Maines. 2000. Neurons overexpressing heme oxygenase-1 resist oxidative stress-mediated cell death. *J. Neurochem.* 75:304–313.

Chen, K., J.A. Vita, B.C. Berk, and J.F. Keaney Jr. 2001. c-Jun N-terminal kinase activation by hydrogen peroxide in endothelial cells involves SRC-dependent epidermal growth factor receptor transactivation. *J. Biol. Chem.* 276:16045–16050.

Chen, K., A. Albano, A. Ho, and J.F. Keaney Jr. 2003. Activation of p53 by oxidative stress involves platelet-derived growth factor-beta receptor-mediated ataxia telangiectasia mutated (ATM) kinase activation. *J. Biol. Chem.* 278:39527–39533.

Cheng, G., Z. Cao, X. Xu, E.G. van Meir, and J.D. Lambeth. 2001. Homologs of gp91phox: cloning and tissue expression of Nox3, Nox4, and Nox5. *Gene.* 269:131–140.

Clempus, R.E., D. Sorescu, A.E. Dikalova, L. Pounkova, P. Jo, G.P. Sorescu, H.H. Schmidt, B. Lassegue, and K.K. Griendling. 2007. Nox4 is required for maintenance of the differentiated vascular smooth muscle cell phenotype. *Arterioscler. Thromb. Vasc. Biol.* 27:42–48.

Dikalova, A., R. Clempus, B. Lassegue, G. Cheng, J. McCoy, S. Dikalov, M.A. San, A. Lyle, D.S. Weber, D. Weiss, et al. 2005. Nox1 overexpression potentiates angiotensin II-induced hypertension and vascular smooth muscle hypertrophy in transgenic mice. *Circulation.* 112:2668–2676.

Djordjevic, T., R.S. BelAiba, S. Bonello, J. Pfeilschifter, J. Hess, and A. Gorlach. 2005. Human urotensin II is a novel activator of NADPH oxidase in human pulmonary artery smooth muscle cells. *Arterioscler. Thromb. Vasc. Biol.* 25:519–525.

Finkel, T., and N.J. Holbrook. 2000. Oxidants, oxidative stress and the biology of ageing. *Nature.* 408:239–247.

Flint, A.J., T. Tiganis, D. Barford, and N.K. Tonks. 1997. Development of "substrate-trapping" mutants to identify physiological substrates of protein tyrosine phosphatases. *Proc. Natl. Acad. Sci. USA.* 94:1680–1685.

Frangioni, J.V., P.H. Beahm, V. Shifrin, C.A. Jost, and B.G. Neel. 1992. The nontransmembrane tyrosine phosphatase PTP-1B localizes to the endoplasmic reticulum via its 35 amino acid C-terminal sequence. *Cell.* 68:545–560.

Frangioni, J.V., A. Oda, M. Smith, E.W. Salzman, and B.G. Neel. 1993. Calpain-catalyzed cleavage and subcellular relocation of protein phosphotyrosine phosphatase 1B (PTP-1B) in human platelets. *EMBO J.* 12:4843–4856.

Geiszt, M., J.B. Kopp, P. Varnai, and T.L. Leto. 2000. Identification of renox, an NAD(P)H oxidase in kidney. *Proc. Natl. Acad. Sci. USA.* 97:8010–8014.

Goyal, P., N. Weissmann, F. Rose, F. Grimminger, H.J. Schafers, W. Seeger, and J. Hanze. 2005. Identification of novel Nox4 splice variants with impact on ROS levels in A549 cells. *Biochem. Biophys. Res. Commun.* 329:32–39.

Haj, F.G., P.J. Verveer, A. Squire, B.G. Neel, and P.I. Bastiaens. 2002. Imaging sites of receptor dephosphorylation by PTP1B on the surface of the endoplasmic reticulum. *Science.* 295:1708–1711.

Haj, F.G., B. Markova, L.D. Klaman, F.D. Bohmer, and B.G. Neel. 2003. Regulation of receptor tyrosine kinase signaling by protein tyrosine phosphatase-1B. *J. Biol. Chem.* 278:739–744.

Halvey, P.J., W.H. Watson, J.M. Hansen, Y.M. Go, A. Samali, and D.P. Jones. 2005. Compartmental oxidation of thiol-disulphide redox couples during epidermal growth factor signalling. *Biochem. J.* 386:215–219.

Hammond, C., and A. Helenius. 1994. Quality control in the secretory pathway: retention of a misfolded viral membrane glycoprotein involves cycling between the ER, intermediate compartment, and Golgi apparatus. *J. Cell Biol.* 126:41–52.

Higashi, H., R. Tsutsumi, S. Muto, T. Sugiyama, T. Azuma, M. Asaka, and M. Hatakeyama. 2002. SHP-2 tyrosine phosphatase as an intracellular target of Helicobacter pylori CagA protein. *Science.* 295:683–686.

Hilenski, L.L., R.E. Clempus, M.T. Quinn, J.D. Lambeth, and K.K. Griendling. 2004. Distinct subcellular localizations of Nox1 and Nox4 in vascular smooth muscle cells. *Arterioscler. Thromb. Vasc. Biol.* 24:677–683.

Kuroda, J., K. Nakagawa, T. Yamasaki, K. Nakamura, R. Takeya, F. Kuribayashi, S. Imajoh-Ohmi, K. Igarashi, Y. Shibata, K. Sueishi, and H. Sumimoto. 2005. The superoxide-producing NAD(P)H oxidase Nox4 in the nucleus of human vascular endothelial cells. *Genes Cells.* 10:1139–1151.

Lee, S.R., K.S. Yang, J. Kwon, C. Lee, W. Jeong, and S.G. Rhee. 2002. Reversible inactivation of the tumor suppressor PTEN by H2O2. *J. Biol. Chem.* 277:20336–20342.

Liu, F., and J. Chernoff. 1997. Protein tyrosine phosphatase 1B interacts with and is tyrosine phosphorylated by the epidermal growth factor receptor. *Biochem. J.* 327:139–145.

Mahadev, K., H. Motoshima, X. Wu, J.M. Ruddy, R.S. Arnold, G. Cheng, J.D. Lambeth, and B.J. Goldstein. 2004. The NAD(P)H oxidase homolog Nox4 modulates insulin-stimulated generation of H2O2 and plays an integral role in insulin signal transduction. *Mol. Cell. Biol.* 24:1844–1854.

Martyn, K.D., L.M. Frederick, K. von Loehneysen, M.C. Dinauer, and U.G. Knaus. 2006. Functional analysis of Nox4 reveals unique characteristics compared to other NADPH oxidases. *Cell. Signal.* 18:69–82.

Meng, T.C., T. Fukada, and N.K. Tonks. 2002. Reversible oxidation and inactivation of protein tyrosine phosphatases in vivo. *Mol. Cell.* 9:387–399.

Menshikov, M., O. Plekhanova, H. Cai, K. Chalupsky, Y. Parfyonova, P. Bashtrikov, V. Tkachuk, and B.C. Berk. 2006. Urokinase plasminogen activator stimulates vascular smooth muscle cell proliferation via redox-dependent pathways. *Arterioscler. Thromb. Vasc. Biol.* 26:801–807.

Pedruzzi, E., C. Guichard, V. Ollivier, F. Driss, M. Fay, C. Prunet, J.C. Marie, C. Pouzet, M. Samadi, C. Elbim, et al. 2004. NAD(P)H oxidase Nox-4 mediates 7-ketocholesterol-induced endoplasmic reticulum stress and apoptosis in human aortic smooth muscle cells. *Mol. Cell. Biol.* 24:10703–10717.

Petry, A., T. Djordjevic, M. Weitnauer, T. Kietzmann, J. Hess, and A. Gorlach. 2006. NOX2 and NOX4 mediate proliferative response in endothelial cells. *Antioxid. Redox Signal.* 8:1473–1484.

Pryor, W.A. 1986. Oxy-radicals and related species: their formation, lifetimes, and reactions. *Annu. Rev. Physiol.* 48:657–667.

Salmeen, A., J.N. Andersen, M.P. Myers, T.C. Meng, J.A. Hinks, N.K. Tonks, and D. Barford. 2003. Redox regulation of protein tyrosine phosphatase 1B involves a sulphenyl-amide intermediate. *Nature.* 423:769–773.

Shiose, A., J. Kuroda, K. Tsuruya, M. Hirai, H. Hirakata, S. Naito, M. Hattori, Y. Sakaki, and H. Sumimoto. 2001. A novel superoxide-producing NAD(P)H oxidase in kidney. *J. Biol. Chem.* 276:1417–1423.

Simpson, R.J. 2003. Differential detergent fractionation of eukaryotic cells. *In* Proteins and Proteomics: a Laboratory Manual. R.J. Simpson. Cold Spring Harbor Laboratory Press, Cold Spring Harbor, NY. 126–135.

Sorescu, D., D. Weiss, B. Lassegue, R.E. Clempus, K. Szocs, G.P. Sorescu, L. Valppu, M.T. Quinn, J.D. Lambeth, J.D. Vega, et al. 2002. Superoxide production and expression of nox family proteins in human atherosclerosis. *Circulation.* 105:1429–1435.

Suh, Y.A., R.S. Arnold, B. Lassegue, J. Shi, X. Xu, D. Sorescu, A.B. Chung, K.K. Griendling, and J.D. Lambeth. 1999. Cell transformation by the superoxide-generating oxidase Mox1. *Nature.* 401:79–82.

Sundaresan, M., Z.X. Yu, V.J. Ferrans, K. Irani, and T. Finkel. 1995. Requirement for generation of H2O2 for platelet-derived growth factor signal transduction. *Science.* 270:296–299.

Thomas, S.R., K. Chen, and J.F. Keaney Jr. 2002. Hydrogen peroxide activates endothelial nitric-oxide synthase through coordinated phosphorylation and dephosphorylation via a phosphoinositide 3-kinase-dependent signaling pathway. *J. Biol. Chem.* 277:6017–6024.

Tonks, N.K. 2003. PTP1B: from the sidelines to the front lines! *FEBS Lett.* 546:140–148.

Touyz, R.M., G. Yao, E. Viel, F. Amiri, and E.L. Schiffrin. 2004. Angiotensin II and endothelin-1 regulate MAP kinases through different redox-dependent mechanisms in human vascular smooth muscle cells. *J. Hypertens.* 22:1141–1149.

Tu, B.P., and J.S. Weissman. 2004. Oxidative protein folding in eukaryotes: mechanisms and consequences. *J. Cell Biol.* 164:341–346.

van Montfort, R.L., M. Congreve, D. Tisi, R. Carr, and H. Jhoti. 2003. Oxidation state of the active-site cysteine in protein tyrosine phosphatase 1B. *Nature.* 423:773–777.

Vaquero, E.C., M. Edderkaoui, S.J. Pandol, I. Gukovsky, and A.S. Gukovskaya. 2004. Reactive oxygen species produced by NAD(P)H oxidase inhibit apoptosis in pancreatic cancer cells. *J. Biol. Chem.* 279:34643–34654.

Wendt, M.C., A. Daiber, A.L. Kleschyov, A. Mulsch, K. Sydow, E. Schulz, K. Chen, J.F. Keaney Jr., B. Lassegue, U. Walter, et al. 2005. Differential effects of diabetes on the expression of the gp91phox homologues nox1 and nox4. *Free Radic. Biol. Med.* 39:381–391.